A configurable dynamometer to evaluate vehicle and battery performance of micromobility devices

Ponaravind Muthaiah [ID],[✉], **Scott Zagorski, Austin Kress, Meredith Bartholomew, Nick Helber, Dale Andreatta and Gary Heydinger**

S-E-A, United States of America

✉ pmuthaiah@sealimited.com

ABSTRACT: The usage of micromobility devices is growing to promote sustainable transportation, prompting manufacturers and regulators to enable its safe integration into urban environments. This has created the need for a tool to evaluate such devices. This paper presents the development of a versatile dynamometer design for verification and validation of micromobility devices by emulating real-world conditions while capturing vehicle and battery performance in real-time. A custom Graphical User Interface (GUI) is used to control and configure the system, as well as enabling the user to analyze and save incoming data. Six devices were chosen from distinct categories to collect data and demonstrate the capabilities and modularity of the dynamometer. The results reflect the ability of the dynamometer to be used for standardized testing of various micromobility devices.

KEYWORDS: Dynamometer, Micromobility, New product development, Mechatronics, Evaluation

1. Introduction

1.1. Micromobility

From 1990 to 2022, CO_2 emissions from transportation have grown on average at 1.7% annually, which is the highest in the end-use sector along with industries (IEA, 2023). In efforts to achieve net-zero emissions by 2050 and limit global warming to 1.5 °C, investments in cleaner energy policies have been increasing, growing 60% across the world in the past four years (IEA, 2024). Promoting sustainable transportation is one such policy to achieve climate goals, which can be made possible by incentivizing the use of public transport in conjunction with micromobility for the first and last mile, provided that the appropriate infrastructure is available for storage (Oeschger et al., 2020). Micromobility has evolved over the years in terms of form factor and mode of power (human, electrical, or electrically assisted), leading to various definitions for the relatively new mode of transportation. The Federal Highway Administration (FHWA) defines micromobility in Price et al. (2021) as

> *Any small, low-speed, human or electric-powered transportation device, including bicycles, scooters, electric-assist bicycles, electric scooters (e-scooters), and other small, lightweight, wheeled conveyances.*

The International Transport Forum (ITF) defines micromobility in Santacreu et al. (2020) as

> *The use of micro-vehicles: vehicles with a mass of no more than 350 kilograms (771 pounds) and a design speed no higher than 45 km/h.*

1.2. Existing research on micromobility

1.2.1. Infrastructure

Urban planners in multiple cities around the world have been working on the infrastructure changes necessary to accommodate the increasing usage of micromobility devices and analyze their viability with existing road networks and traffic patterns. To support these efforts, researchers have proposed design changes to increase the safety of riders, providing routing options alongside bicycle lanes to reduce the risk of accidents (Ignaccolo et al., 2022; Hossein Sabbaghian et al., 2023; Folco et al., 2023).

1.2.2. Energy efficiency

Stilwell et al. (2023) elaborates on the role of e-scooter tire selection in energy efficiency by building a test rig and evaluating coast-down distances of seven e-scooter tires. Stilwell et al. (2024) developed a rolling resistance trailer to analyze the resistive forces of nine e-scooter tires and reinforced the need for better design choices to reduce the environmental impact of e-scooters.

1.2.3. Rider behavior

Garman et al. (2020) equipped an e-scooter and riders of varying percentiles with sensors to collect data on vehicle performance and rider kinematics to observe the effect of rider position on braking distance. Dozza et al. (2023) used sensor fusion to collect vehicle data for a variety of velocity profile tests using riders of distinct experience levels with micromobility devices to conclude that rider behavior and safety differ among an e-scooter, bicycle, and Segway.

1.2.4. Cybersecurity

Hilgert et al. (2021) analyzed the applications of a few micromobility service providers looking at their methods for storing and retrieving user, ride, and payment information. They also explore the possibilities of accessing such information through each provider's Application Programming Interface (API). In some instances, creating spoofed user trips using a valid e-scooter license plate was found to be possible. Vinayaga-Sureshkanth et al. (2020) provided an overview of existing and potential security vulnerabilities, their consequences, and corresponding countermeasures in urban micromobility space.

1.3. Need for verification and validation of micromobility devices

The usage of micromobility devices is growing every year. In the U.S. and Canada, 157 million shared micromobility trips were taken in 2023 compared to 92 million trips in 2018 (NACTO, 2024). This rapid increase in usage escalated the issues with the manufacturing of micromobility devices and the urgent need for extensive testing. After receiving reports of at least 208 fire or overheating incidents from micromobility devices between 2021 and 2022, the U.S. Consumer Product Safety Commission (CPSC) called for micromobility devices manufactured in the U.S. and imported from other countries to comply with UL 2272 – Standard for Electrical Systems for Personal E-Mobility Devices and UL 2849 – Standard for Safety for Electrical Systems for eBikes (CPSC, 2022). These standards, along with other standards like UL 2271 - Standards for Batteries in Light Electric Vehicles, provide guidance for manufacturers to verify that their devices meet the requirements and for regulators to validate if the devices on the market comply with those standards and further assess the risk that these devices possess for consumers.

1.4. Contributions of this paper

While there is a considerable amount of research towards enabling the peaceful co-existence of micromobility devices alongside motorized vehicles and pedestrians, there is a clear vacuum in the research of evaluating micromobility devices to meet safety standards. This paper aims to address that vacuum by detailing the steps involved in building a dynamometer, as a tool for manufacturers and regulators to verify and validate micromobility devices. Figure 1 shows the design of the dynamometer equipped with a hoverboard to be evaluated. The core capabilities of the dynamometer are as follows:

(1) Versatile design that accommodates a variety of electric micromobility devices such as kick scooters, bicycles, skateboards, hoverboards, unicycles, and youth All-Terrain Vehicles (ATV).

(2) Emulate road loading up to 12.5 lb-ft using rollers of 6 inch diameter and rider loading up to 400 lbf using electronically controlled brakes and actuators.

(3) Measure vehicle and battery performance characteristics consistently under variable test conditions.

(4) Real-time Data Acquisition (DAQ) that can monitor more than 70 channels simultaneously.

2. System overview
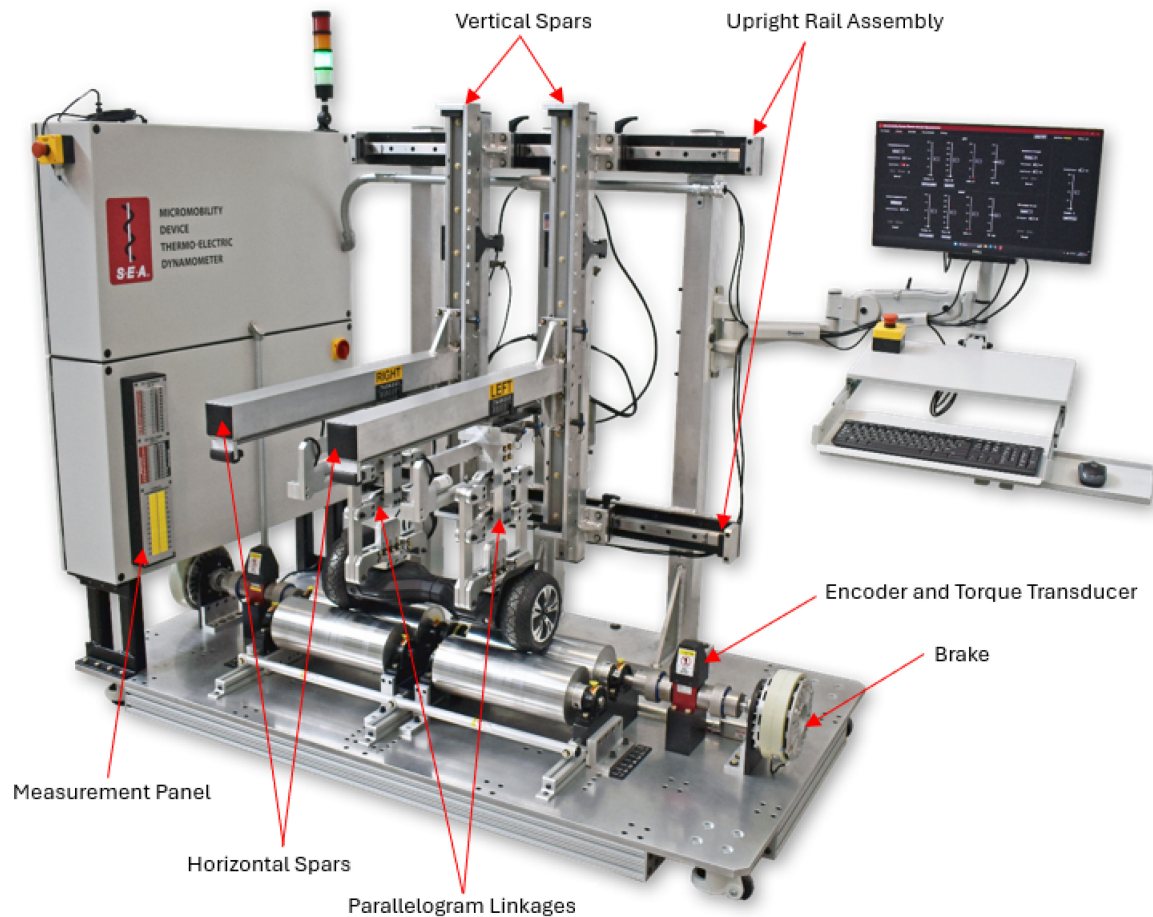
**Figure 1. Micromobility Device Dynamometer with a Hoverboard**

2.1. Road load

To emulate forces that resist the motion of micromobility devices on road, a pair of rollers is placed on a shaft in line with the speed encoders, torque transducers, and brakes, while a pair of idler rollers rotate freely on a shaft parallel to the main rollers. The two pairs of rollers, along with the brakes, collectively enable micromobility devices to achieve the desired speed and road load set by the user during test runs by positioning the device's wheels in between the main and idler rollers. Simulated road loads are measured using torque transducers and are tuned by setting the amount of resistance provided by the brakes. For devices that do not have independently driven left and right wheels, the main rollers can be coupled using a two-part coupling mechanism. The idler rollers can be moved on the rail system to accommodate devices of varying tire sizes. Using this set-up, a road load of up to 12.5 lb-ft can be emulated using rollers of 6 inch diameter.

2.2. Rider load

Micromobility devices are secured on the dynamometer using vertical and horizontal spars. The two vertical spars are manually adjusted based on the width of the device to be tested by moving them laterally on the upright rail assembly. Once adjusted, the vertical spars are locked in position using the

brake-handles provided. The horizontal spars are adjusted based on the height of the device coarsely (within 4 inches with manual adjustment) and then using linear actuators through the GUI. Upon contact with the device, variable pressure can be applied using the actuators to emulate a maximum rider load of 400 lbf per actuator. Figure 2(a) shows the right linear actuator with its load cell used to monitor rider load.
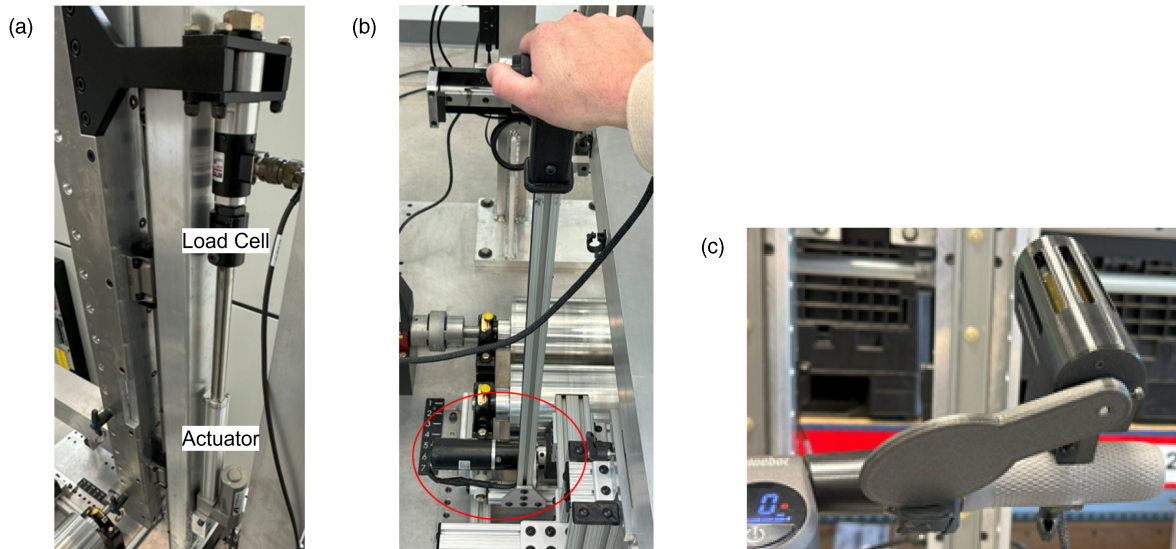
Figure 2. (a) Linear actuator with load cell, (b) Kickstart motor, (c) Throttle motor

2.3. Kickstart and throttle control

Selected micromobility devices, such as kick scooters, may require the user to place one foot on the scooter and give an initial push forward using the other foot on the ground as a prerequisite to enable throttle after reaching speeds of 2-3 mph. To emulate this initial momentum, a kickstart motor is used in contact with the idler roller, as shown in Figure 2(b). Once the kick scooter achieves the desired speed, the user can input desired throttle using the GUI, resulting in the lever applying appropriate force on the kick scooter's throttle switch as shown in Figure 2(c). The lever can rotate 360°, supporting various placements of the throttle switch in different devices. This combination of kickstart and throttle control enables the user to achieve kickstart speeds up to 3 mph and then electronically perform speed control after the device's motor begins operating.

2.4. Tilt motion control

Micromobility devices such as hoverboards require users to lean forward or backward to control the speed and acceleration of the device. Linear actuators mounted on parallelogram linkages resting on the device as shown in Figure 3(a) provide the user with the means to emulate the tilt motion of a rider and accelerate or decelerate the device. This is accomplished by giving the desired tilt as input through the GUI during the test, which in turn extends or retracts the linear actuator, enabling the device to tilt a maximum of $\pm 30°$ on either side of its axis of rotation.

2.5. Current, voltage and temperature measurements

The measurement panel placed on the electronics box as shown in Figure 3(b) has 12 current channels for up to 50 ADC, 12 voltage channels for up to 150 VDC, and 24 temperature channels for Type-K thermocouples. The current, voltage, and temperature of components in a micromobility device, such as the battery among other electronics, can be measured by connecting wires from the device to the appropriate ports on the panel. The user can monitor and collect such data during the test period using the GUI.
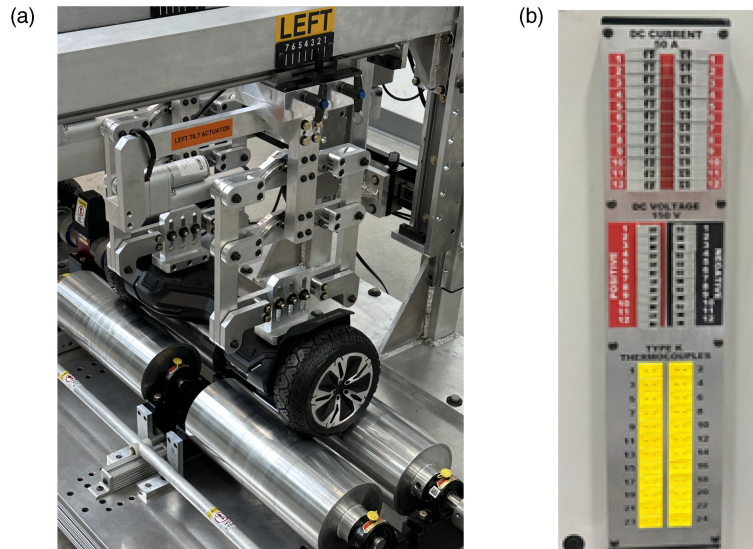
(a)

(b)

Figure 3. (a) Tilt actuators on parallelogram linkages, (b) Measurement panel
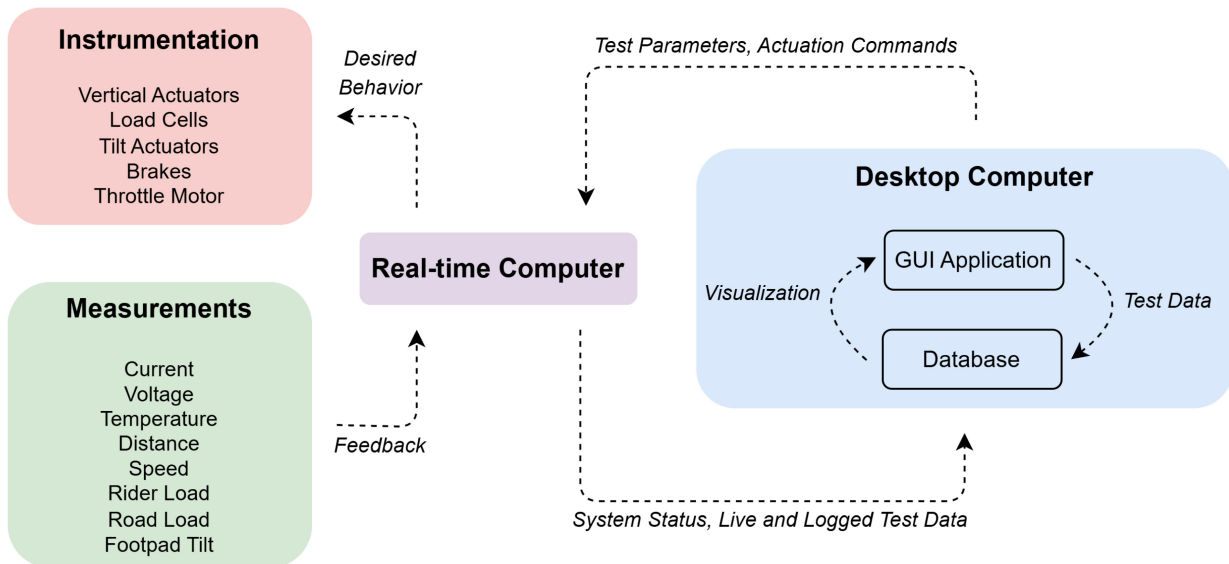
3. Software architecture

Figure 4. Software architecture

3.1. Real-time Data Acquisition (DAQ)

A NI Compact Reconfigurable Input/Output Module (cRIO) with a Linux Real-Time Operating System (RTOS) is chosen as the real-time computer, directly connected to a Field Programmable Gate Array (FPGA) for better performance, programmed with LabVIEW. The real-time computer communicates with the dynamometer's instrumentation, sensors and desktop computer as shown in Figure 4. The GUI application on the desktop computer communicates through Transmission Control Protocol (TCP) with the real-time computer to relay the user-input test parameters and system configurations prior to the start of the test. The actuation commands are also communicated if both computers are connected, with the desktop computer acting as a client and the real-time computer acting as the server. These actuation commands are translated into desired behavior for instrumentation, such as actuators, motors, and load cells. Based on the requested behavior, the real-time computer collects feedback to control the instrumentation as the test progresses and to log real-time test data. The real-time computer also

communicates through TCP to let the GUI application know the dynamometer's status along with live measurements for visualization.

3.2. Graphical User Interface (GUI)

The GUI application is hosted on a Windows 11 desktop computer in conjunction with the database. The GUI is a Windows Presentation Foundation (WPF) application based on the.NET platform, developed using C# and Extensible Application Markup Language (XAML). The user utilizes the GUI application to input test parameters, control the dynamometer, visualize live and prior test data, and adjust system configurations. During the test, user commands are added to a queue and sent to the DAQ to be processed. The GUI also processes incoming live readings and visualizes it for the user. At the end of each test, if the user chooses to save the test data, the GUI application transfers logged measurements to the desktop computer using Web Distributed Authoring and Versioning (WebDAV) and saves to the database, which can also be visualized in the recorded data tab of the GUI. Microsoft Access is used as a Structured Query Language (SQL) based data source for storing and retrieving test data by the GUI using the Object Linking and Embedding Database (OLEDB) API. A screenshot of the recorded data tab on the GUI is shown in Figure 5.
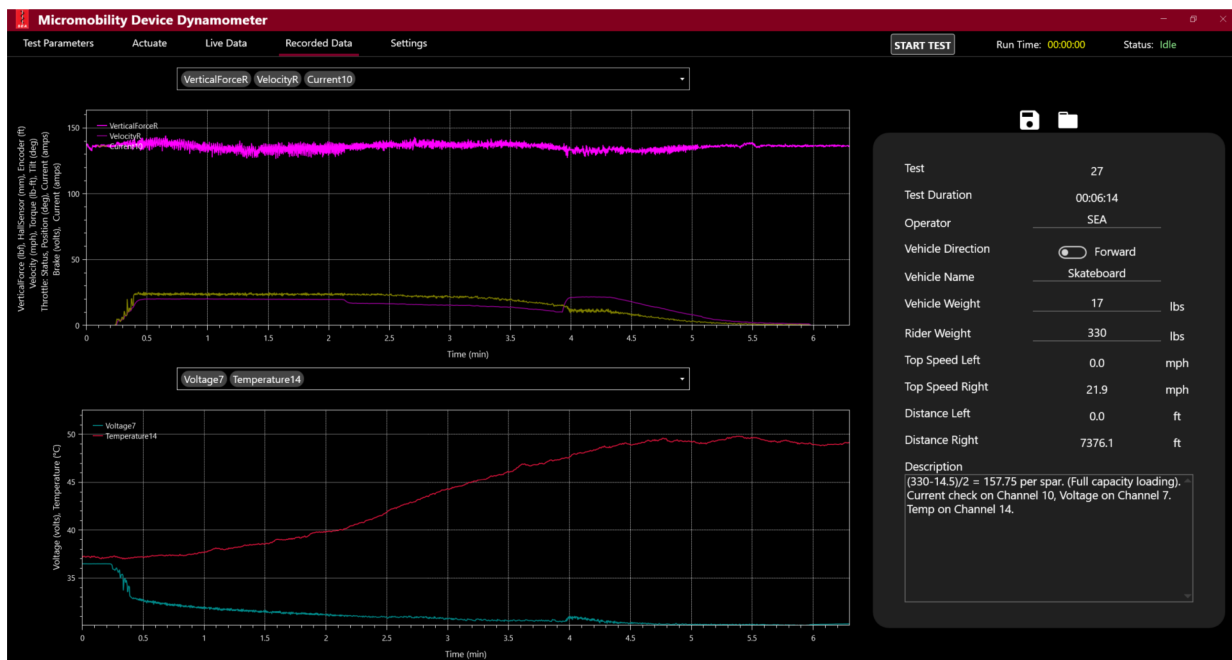

Figure 5. Recorded data tab on the GUI

4. Test methodology

4.1. Device selection

Six devices were chosen across multiple categories with varying tire diameter, load capacity and mode of operation. The parameters for the chosen devices are listed in Table 1.

4.2. Test setup

Based on the tire size (d) of the device, the idler rollers were adjusted to achieve a contact angle (θ) of 30° resulting in the desired roller spacing (x) as illustrated in Figure 6. The left and right rollers were coupled only for the bicycle and the youth ATV to enable braking to be distributed between the left and right brakes, while other devices were tested with decoupled rollers. The horizontal spars were adjusted by moving on the upright rail assembly to suit the width of device to be tested. The hoverboard and youth ATV were secured on both left and right rollers, while the other four devices were secured on one side of

Table 1. Device parameters.

Category	Model	Tire Diameter (inches)	Max Rider Load (lbs)	Speed Control	Kickstart
Hoverboard	Gyroor G2	8.5	256	Tilt	No
Unicycle	Gosmilo X1	11	265	Tilt	No
Bicycle	Heybike Ranger S	20	400	Throttle	No
Skateboard	Meepo V5	3.5	330	Handheld	No
Kick scooter	Ninebot ES2	8	220	Throttle	Yes
Youth ATV	Razor Dirt Quad 500	14.5	220	Throttle	No

icle performance time series data for 6 devices. (a-b) velocity, (c-d) distance, (e-f) rider load, (g-h) road load

the dynamometer, using one main and one idler roller. The parallelogram linkages shown in Figure 3(a) were attached for devices such as hoverboard and unicycle which require tilt motion to be emulated. The vertical spars were lowered using the actuators to match the height of the device to be tested. For devices requiring throttle control such as the kick scooter, bicycle, and youth ATV, the throttle motor was mounted on the handle as shown in Figure 2(c). Minimum and maximum throttle limits for each device were set by the user through the GUI prior to the test. A lift table was used to support the non-driven wheels of any device. Additionally, to demonstrate the dynamometer's ability to measure battery performance under load, the skateboard's battery was wired to the current, voltage, and temperature ports on the measurement panel.
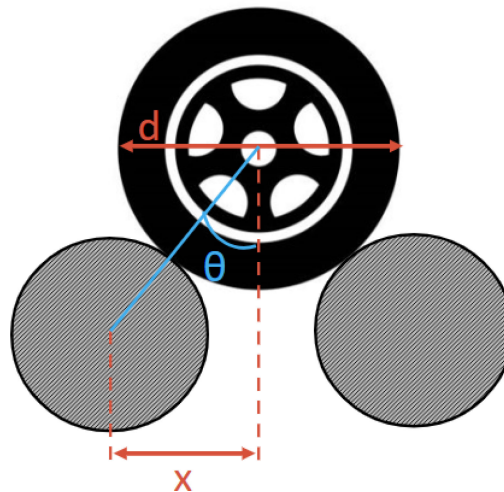
Figure 6. Roller spacing

4.3. Test procedure

Desired rider load and road load were applied to the device using the GUI. To vary the test parameters used for each device, a matrix of various combinations of rider load and road load was used. The data sampling rate was set at 10 ms for all devices. The kickstart motor shown in Figure 2(b) was used to get the kick scooter to 3 mph and enable its motor through the Electronic Control Unit (ECU). The throttle motor was used to adjust the throttle on the kick scooter, bicycle, and youth ATV. The skateboard's speed was controlled using the manufacturer provided handheld remote. Once test parameters and system configurations were set by the user, data recording was initiated and desired velocity was achieved using the tilt actuators or throttle motor depending on the device being tested. The test duration for the six devices ranged between 6 minutes to 28 minutes depending on the battery capacity of the device, rider load and road load applied.

5. Results
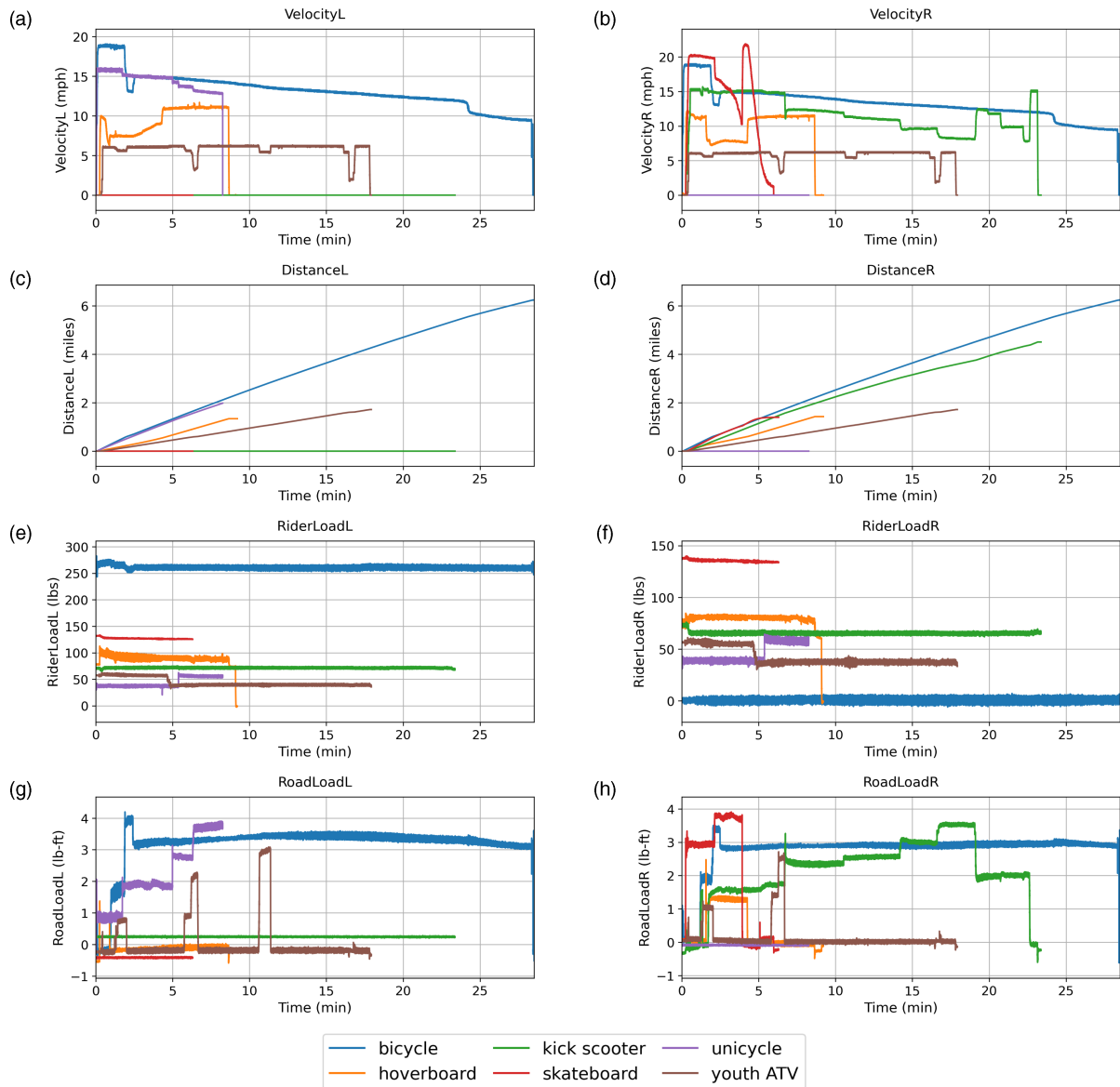
Figure 7. VehTable

The plots shown in Figure 7 are reflective of the user's desired parameters and actuation on the left and right side of the dynamometer for the entire test duration. The distance traveled by the devices were measured using encoder counts converted to miles, velocities were measured by the rate of change of encoder counts converted to miles per hour, rider load was measured by the load cell on the vertical actuators shown in Figure 2(a), and road load was measured by the torque transducer. The kick scooter and skateboard have no velocity and distance data on the left as it was mounted on the right. Similarly, the unicycle has no velocity and distance data on the right as it was mounted on the left side of the dynamometer. The bicycle and youth ATV have equal velocities and distance traveled on left and right as the rollers were coupled for those devices. A moving average filter was used to reduce the noise in rider load and road load data. The rider load fluctuations seen in Figure 7 (e) and Figure 7(f) are a result of the load cells capturing the up and down motion of the devices under desired load and velocity. The road load fluctuations observed in Figure 7(g) and Figure 7(h) were derived from the torque transducers under the same test conditions. Figure 8(a), Figure 8(b), and Figure 8(c) depict typical battery discharge behavior during usage on the skateboard as the current drawn increases with speed, whereas a drop in voltage and rise in temperature can be seen as the test progressed.
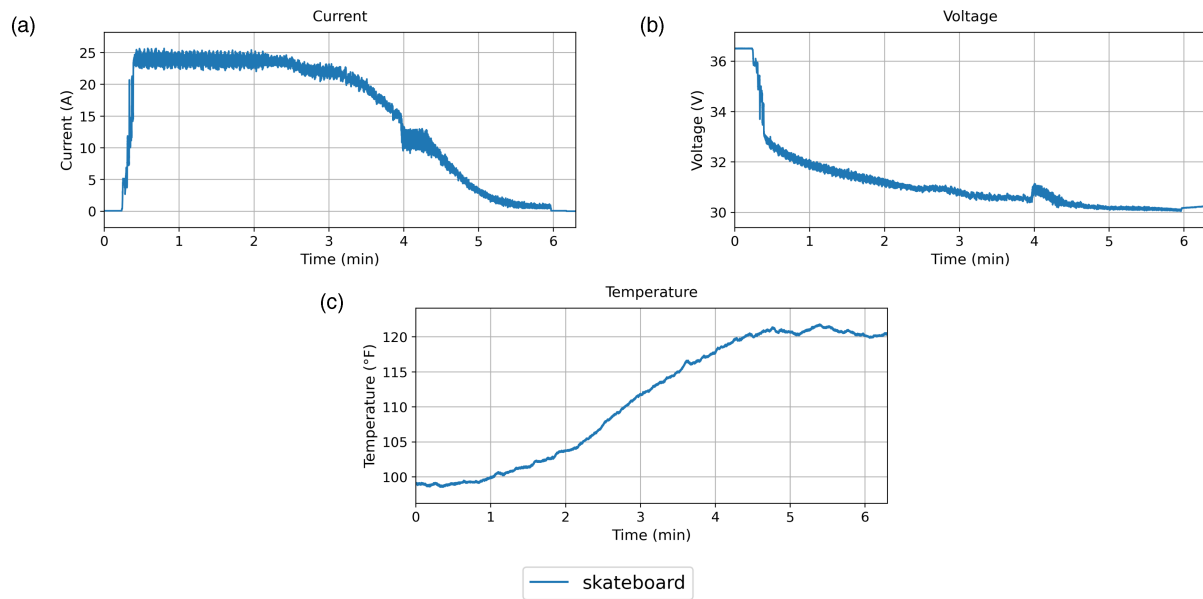
Figure 8. Battery performance time series data for skateboard. (a) current, (b) voltage, (c) temperature

6. Conclusions

The micromobility device dynamometer presented in this paper provides a foundation for manufacturers and regulators, enhancing the standardized evaluation of vehicle and battery performance by emulating real-world conditions. The results demonstrate its capability as a versatile tool for various micromobility devices by effectively gathering real-time data through instrumentation, sensors, and software. The vehicle performance test results showed the user's ability to effectively control the velocity, rider load, and road load of all six devices. The battery performance test results revealed a natural discharge pattern with expected correlations between current draw, voltage decline, and temperature increase. These results provide valuable insights for the testing organization about vehicle and battery behavior under a variety of probable real-world conditions to evaluate the robustness of the device under test. Future developments could include additional performance metrics and evaluation of a larger collection of devices. For example, different electric bicycles could be tested against each other under different loading conditions to determine battery performance.

References

International Energy Agency (2023). Tracking Clean Energy Progress 2023. *IEA*.

International Energy Agency (2024). State of Energy Policy 2024. *IEA*.

Oeschger, G., Carroll, P. and Caulfield, B. (2020). Micromobility and public transport integration: The current state of knowledge. *Transportation Research Part D: Transport and Environment*, 89, 102628.

Price, J., Blackshear, D., Blount Jr, W. and Sandt, L. (2021). Micromobility: A travel mode innovation. *Public Roads*, 85(1).

Santacreu, A., Yannis, G., de Saint Leon, O. and Crist, P. (2020). Safe micromobility. *International Transport Forum*, Paris.

National Association of City Transportation Officials (2024). 2023 Shared Micromobility in the U.S. and Canada report. *NACTO*.

U.S. Consumer Product Safety Commission (2022). CPSC Calls on Manufacturers to Comply with Safety Standards for Battery-Powered Products to Reduce the Risk of Injury and Death. *CPSC*.

Stilwell, G., Gooch, S., Goodwin, M. and Zarifeh, H. (2023). Evaluation of e-scooter tyre performance using dynamometer-based coast-down tests. *Proceedings of the Design Society*, 3, 1695–1704.

Stilwell, G., Gooch, S. and Lafitte, M. (2024). Comparison of e-scooter tyre performance using rolling resistance trailer. *Proceedings of the Design Society*, 4, 1457–1466.

Garman, C.M.R., Como, S.G., Campbell, I.C., Wishart, J., O'Brien, K. and McLean, S. (2020). Micro-mobility vehicle dynamics and rider kinematics during electric scooter riding. *SAE Technical Paper*, 2020-01-0935.

Hilgert, J.-N., Lambertz, M., Hakoupian, A. and Mateyna, A.-M. (2021). A forensic analysis of micromobility solutions. *Forensic Science International: Digital Investigation*, 38, 301137.

Dozza, M., Li, T., Billstein, L., Svernlöv, C. and Rasch, A. (2023). How do different micro-mobility vehicles affect longitudinal control? Results from a field experiment. *Journal of Safety Research*, 84, 24–32.

Vinayaga-Sureshkanth, N., Wijewickrama, R., Maiti, A. and Jadliwala, M. (2020). Security and privacy challenges in upcoming intelligent urban micromobility transportation systems. In: *Proceedings of the Second ACM Workshop on Automotive and Aerial Vehicle Security*, March 2020, pp. 31–35.

Ignaccolo, M., Inturri, G., Cocuzza, E., Giuffrida, N., Le Pira, M. and Torrisi, V. (2022). Developing micromobility in urban areas: network planning criteria for e-scooters and electric micromobility devices. *Transportation Research Procedia*, 60, 448–455.

Hossein Sabbaghian, M., Llopis-Castelló, D. and Garca, A. (2023). A safe infrastructure for micromobility: the current state of knowledge. *Sustainability*, 15(13), 10140.

Folco, P., Gauvin, L., Tizzoni, M. and Szell, M. (2023). Data-driven micromobility network planning for demand and safety. *Environment and Planning B: Urban Analytics and City Science*, 50(8), 2087–2102.